EXPLOITING SUNGLINT SIGNATURES FROM MERIS AND MODIS IMAGERY IN COMBINATION TO SAR DATA TO DETECT OIL SLICKS

M. Adamo[1], G. De Carolis[2], V. De Pasquale[2], and G. Pasquariello[2]

[1]*Dept. of Physics, University of Bari, 70126 Bari, Italy*
[2]*Institute of Intelligent Systems for Automation, National Research Council, 70126 Bari, Italy*

ABSTRACT

SAR spaceborne capability to detect marine oil spills through the damping of wind generated short gravity-capillary waves has been extensively demonstrated during the past years. In contrast, it has not yet been found any suitable method which exploits VIS/NIR imagery supporting SAR observations. To this end, we propose the use of MODIS and MERIS images acquired in sunglint conditions to reveal smoothed regions such as those affected by oil pollution. The underlying physical mechanism is based on the modification of the surface slopes distribution composing the roughened sea due the action of mineral oils. The methodology is demonstrated for a case study in the Mediterranean Sea where spills were detected by ASAR imaging.

Key words: oil spill; SAR; MODIS; MERIS; sunglint.

1. INTRODUCTION

Oil spills in the marine environment is the cause of major pollution problems of the sea surface. The knowledge of the present position of spilled oil and the ability to predict its motion are essential components of successful oil spill response. These functions are known as surveillance and tracking. Synthetic aperture radar (SAR) images gathered by ERS-1, ERS-2, RADARSAT satellites have been extensively used to obtain statistical information on oil polluted areas. SAR capability to acquire images of the Earth surface independent of solar illumination, cloud coverage and atmospheric conditions, stimulated research programs to develop methods for accurate oil spill detection. The operative use of spaceborne SAR imagery is however limited by the low revisiting period of acquisition of the same area (about 30 days), thereby hindering the possibility to follow the movement of the spilled oil on the sea surface.
The aim of this paper is to propose the use of SAR data with additional satellite information gathered at higher temporal rates, such as visible/near-infrared (VIS/NIR) satellite imaging sensors, to follow the oil spill during its life. The VIS/NIR sensors guarantee a revisiting time of the order of one day or less, but they are limited by solar illumination for optical bands and require clear sky for surface imaging. Besides, up to now their potential to detect marine oil spills has been limited by their coarse spatial resolution. In contrast, the latest multispectral VIS/NIR sensors can acquire images at suitable spatial resolution (less than 300 m) for oil spill detection.
Up to now, the VIS/NIR features to be exploited for oil spill identification has been focused on the search of any spectral signatures, distinctive of mineral oils, to be used as a tool to discriminate clean water from oil polluted water. The latter approach is thus limited by the strong condition that the return signal was not contaminated by sunglint. Indeed, the signal reflected by the sea surface always contains a certain percentage of sunglint, thereby the use of spectral information at VIS/NIR frequencies could be useful only for very particular imaging conditions. In this paper we exploit information gained by sunglint imaging to manifest the changes of sea surface roughness caused by the damping action of the mineral oil upon the capillary-short gravity waves.

2. THE SEA SURFACE REFLECTANCE

2.1. Theoretical description

Sunglint is the direct specular reflection of the solar radiation over the ocean waves. As a result, the typical image of a sea surface portion acquired in sunglint condition is brighter than the surrounding region. The physical description of sunglint reflectance of the sea surface can be carried out on statistical basis. Cox & Munk [1][2] showed that the sea surface can be represented as a collection of small, mirror-like planar facets each with a characteristic slope. A large portion of the sea surface can thus be described by means of a statistical slopes' distribution as a function of the horizontal wind vector. From the knowledge of the slopes' distribution, sunglint reflectance can be computed as a composite of contributions from facets oriented as a mirror with respect to the observation point where the sensor is located.
In a local, target-fixed, three-dimensional Cartesian coordinates system whose y-axis is aligned with the sun azimuth, to each facet composing the sea surface can be

Proc. 'Envisat Symposium 2007', Montreux, Switzerland
23–27 April 2007 (ESA SP-636, July 2007)

assigned the slope components (z_x, z_y). The probability that the facet reflects specularly the incident solar radiation to the sensor position depends on the wind speed W and wind direction ϕ. If the sun system (x, y) is rotated toward the wind direction, the probability distribution reduces to a simplified Gram-Charlier form of a 2D Gaussian distribution [1]. For its expression, we refer the reader to formula (18) and subsequent formulas of the earlier paper by Cox & Munk [1].
The sunglint reflectance can be readily expressed as follows [1]:

$$\rho_G = \frac{\pi}{4} \frac{r(\omega, \lambda)}{\cos\theta_s \cos\theta_v \cos^4\beta} p(z_x^{'}, z_y^{'}) \qquad (1)$$

where $(z_x^{'}, z_y^{'})$ are the facet's slope components in the wind system and ω is the specular reflection angle. θ_s and θ_v are the sun and sensor zenith angles; β is the angle formed by the facet normal and z-axis; finally, $r(\omega, \lambda)$ is the Fresnel reflection coefficient at radiation wavelength λ, which is almost constant (0.02) for angles between 0 and 50 degrees.

2.2. Atmospheric contribution

Remote sensing from VIS/NIR satellite sensors is strongly affected by the presence of the atmosphere along the paths connecting sun - sea surface - sensor. Therefore, the atmospheric contribution to the VIS/NIR decay should be suitably modelled for accurate radiance measurements from spaceborne sensors.
There are two chief atmospheric processes that modify the solar radiance reflected from the sea surface when it is viewed from the space: the absorption by atmospheric gases and the scattering by aerosols and molecules. A comprehensive description of the radiation field in the atmosphere, which allows the computation of the reflectance at the top of the atmosphere (TOA), can be obtained from the radiative transfer equation (RTE) [3].
No analytical solutions exist for the RTE, but various approximate solutions are available, among which the vectorial radiative transfer code "6S" considered for this study [4]. In 6S the equation of transfer is solved using successive order of scattering approximation (SOS) for vertical inhomogeneous atmosphere. The reflectance at TOA, ρ_{toa}, can thus be computed using an expression which includes:

- a term representing the reflectance contribution of the atmosphere if the sea surface was perfectly absorbent;
- a term that takes into account the reflectance of the foam and of the water in the Lambertian (isotropic) approximation;
- a term representing the reflectance contribution of the photons that directly impinge the sea surface from the sun and are reflected to the sensor;
- a term describing the photons spread by the sea surface, specularly reflected and directly transmitted to the sensor;
- a term describing the photons directly transmitted to the sea, specularly reflected and diffusely transmitted to the sensor;
- two terms which take into account photons that are diffusely transmitted to the sea, reflected and diffusely transmitted to the sensor [5].

To run the 6S code, several parameters must be defined. Besides the geometrical and spectral imaging conditions, the vertical profile and the properties of the atmosphere should be carefully specified.
To carry on this study, a small area near the oil spill was selected and the atmospheric parameters corresponding to each pixel belonging to the area were computed to determine the TOA reflectance. Aerosol characterization was performed using a procedure that exploits the SWIR bands of MODIS [6]. As MERIS sensor does not have SWIR imaging capability, the nearest temporal MODIS image has been considered to retrieve aerosol properties relevant to the actual MERIS acquisition.

3. EXPERIMENTAL RESULTS

The following procedure has been set up to demonstrate the use of sunglint VIS/NIR imagery to support SAR observations of oil slicks. High resolution MODIS products (250 m nadir resolution) and MERIS imagery (300 m nadir resolution) affected by sunglint signature are selected for the days around the date of SAR oil slick detection. The analysis is performed using the band 2 (841-876 nm) of MODIS and the band 13 (855-875 nm) of MERIS as they were found the most sensitive wavelength intervals for the detection of the sea surface properties. Then, the following steps are taken to analyze signatures on VIS/NIR imagery:

1. Slick localization after image geo-referencing and stretching;
2. Generation of sunglint reflectance image using expression (1) and comparison to TOA image reflectance by calculating the ratio

$$R = \frac{\rho_{toa}}{\rho_G} \qquad (2)$$

In order to compute surface reflectance, knowledge of 10 m wind speed and direction is needed. The latter can be estimated by inversion of calibrated SAR backscatter using the semi-empirical backscatter model CMOD4. Surface wind vectors predicted by the atmospheric model operational at ECMWF is considered as guess input to SAR wind inversion procedure [7]. Alternatively, the surface

Table 1. List of the analyzed image dataset.

Date	Time	Sensor
30/08/2004	09.00 a.m.	MODIS Terra
31/08/2004	08.43 a.m.	MERIS
31/08/2004	11.20 a.m.	MODIS Aqua
02/09/2004	09:35 a.m.	MODIS Terra
03/09/2004	08:48 a.m.	MERIS
03/09/2004	08:02 p.m.	ASAR
04/09/2004	08.17 a.m.	ASAR
04/09/2004	09.20 a.m.	MODIS Terra
04/09/2004	10.55 a.m.	MODIS Aqua

wind vector provided by ECMWF is exploited if the temporal distance between SAR and VIS/NIR imagery exceeds the three hours, i.e. half the scheduled temporal interval of ECMWF outputs.

The procedure described before has been applied to a case of oil slick localized about 200 Km South of the Eastern part of Crete island as documented by the ASAR Wide Swath image acquired on 4th September 2004 at 8:17 UTC. The MODIS Terra and MODIS Aqua images, acquired over the same area at 9:20 and 10:55 UTC on the same day, were found affected by important sunglint signature. Both images reveal the slick detected by ASAR (Figure 1). The MODIS Aqua image of the slick appears broken into three pieces. This is an artifact frequently observed on MODIS images, which exhibit the effects of mirror side and inter-detector banding.

By extending the search of sunglint VIS/NIR images up to one week before and after the ASAR acquisition date, two probable oil slicks have been detected in the same geographic area. They were picked up by the MODIS Terra image acquired on 30th August 2004 at 9.00 UTC, by the MERIS and MODIS Aqua images acquired on 31st August 2004, at 8.13 UTC and 11.20 UTC respectively (Figure 2). It should be pointed out that the ASAR WS image gathered the day before (3rd September, 8:02 pm) the discovery of the slick under study did not show any slick features. Similarly, the MERIS image acquired on 3rd September and the MODIS Terra acquired on 2nd September, both showing sunglint signatures, did not document any presences of slicks. Details about the complete dataset are summarized in the Table 1.

The newly discovered probable oil slicks have almost different shapes. The first slick has a stable threadlike shape on all the images, while the second one shows a changing angular shape over the next 26 hours.

In order to estimate the feasibility of the proposed method, a separability index able to quantify the discrimination capability between the oil polluted pixels and the surrounding pixels has been considered. The separability index is computed on the TOA reflectance image and on the previously defined R image (see expression 2), respectively. In order to evaluate the impact of the atmospheric effects on the detection capability of slicks by

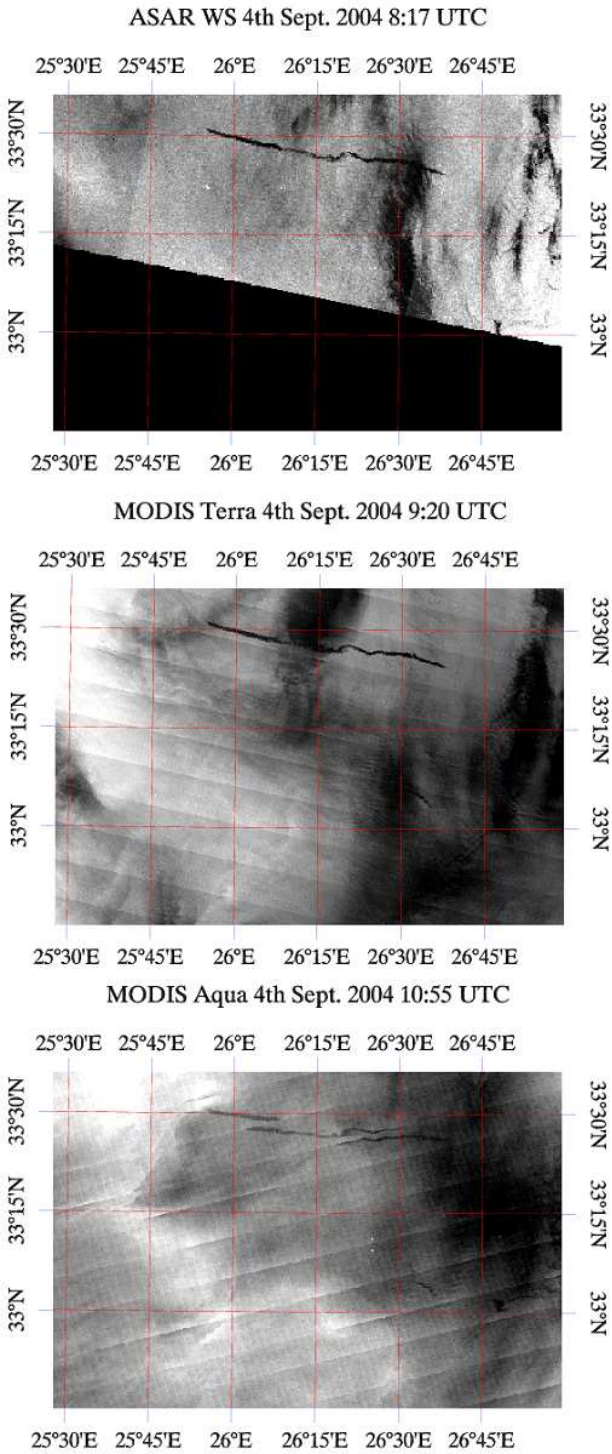

Figure 1. A threadlike oil slicks near Crete detected by ENVISAT ASAR, MODIS Terra and MODIS Aqua on 4th September 2004.

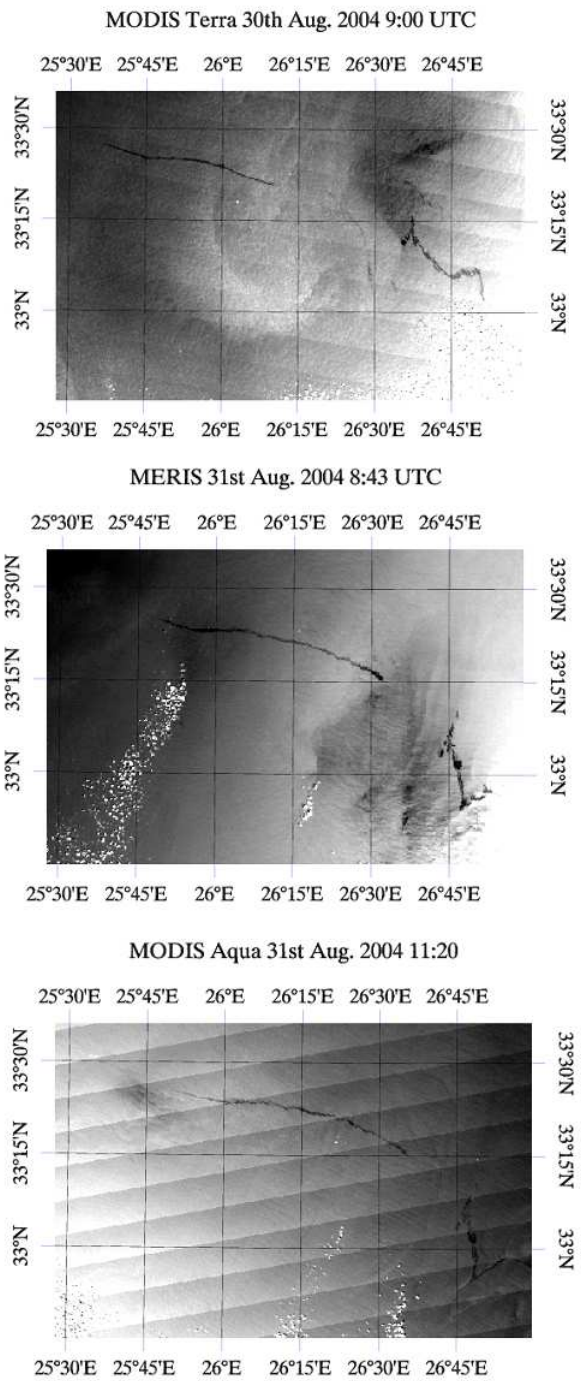

Figure 2. A threadlike and angular oil slicks near Crete detected by MODIS Terra, MERIS and MODIS Aqua from 30th to 31st August 2004.

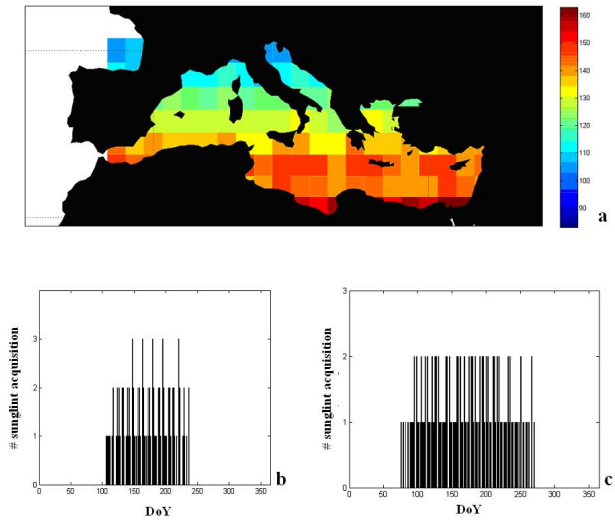

Figure 3. Number of sunglint acquisition during 2006 considering MERIS, MODIS Terra and MODIS Aqua sensors for the Mediterranean Sea (a), temporal distribution of the sunglint acquisitions for an area localized in the northern part of the Adriatic Sea (b) and offshore Crete (c).

VIS/NIR images, the separability index was also computed by defining a new R image as the ratio between the image reflectance at TOA and the 6S simulated TOA reflectance. Assuming that the pixel values both belonging to the oil slick and to the background region are normally distributed, whatever the reflectance or R's images are concerned, the separability index S of the pixel ensembles can be expressed as:

$$S = \frac{|M_{oil} - M_{bg}|}{\sigma_{oil} + \sigma_{bg}} \tag{3}$$

where (M_{oil}, σ_{oil}) and (M_{bg}, σ_{bg}) are the parameters of the Gaussian distribution describing the oil slick and background region respectively. The measurements carried out on the above mentioned detected "probable" oil slicks show that, on average, the slicks are enhanced with respect to the background (i.e., S index is higher) by using R images. Furthermore, in most cases S index increase if the atmospheric contribution is taken into account. The latter is an expected result because the atmospheric contributions are homogeneously taken into account into the "6S" simulated reflectance image. The decreased performances could thus be attributed to a poor evaluation of the atmosphere constituents as done by the 6S code.

3.1. Method applicability

The proposed methodology can be successful applied provided the sunglint conditions are fulfilled by the imaging optical sensors. It results that the mid-latitude seas, such as the Mediterranean Sea, are the candidate regions for best performances. We therefore carried out extensive

simulations over the Mediterranean Sea to determine both the number of sunglint occurrences and the temporal extent during the year 2006 for the sensors aboard the satellites ENVISAT, AQUA and TERRA. Simulations were carried out over a 2' separation grid assuming an average wind speed of 5 m/s and no cloud coverage. Figure 3a represents the map of the cumulative number of acquisitions in sunglint for the three sensors. As expected, going through the north, the number of useful acquisitions decreases as a result of the increasing less favourable sun–sensor relative positions.
In Figure 3b and Figure 3c the temporal distribution of sunglint acquisitions for a point localized in the Northern Adriatic Sea and offshore Crete are respectively shown. The plots shows that the period covering the spring to the early autumn guarantees a suitable probability to image the point in sunglint condition. Besides, it should be pointed out that this period reduces considering northern areas.

3.2. The tracking of oil slick

The chief application of the procedure described above is the possibility to track an oil slick.
Referring to the slicks' features observed in Figure 2, there are important differences relevant to the position and the shape of the slicks during the about 24 hours lagging the MODIS Terra and MERIS acquisitions. In contrast, almost no differences can be captured on the MERIS and MODIS Aqua images as a result of the short time (about 2.5 hours) separating the two acquisitions. Due to the variation in the shape of the angular slick, accurate estimation of its movement is a rather difficult task. However, by selecting some points belonging to the slick so that they are present in all images, a movement of about 17 km between the first two acquisitions and about 3 km between the last two can be estimated. These distances correspond to an average slick velocity respectively of 0.21 m/s and 0.3 m/s. As the average wind speed was about 5 m/s, the long term slick velocity is about 4% the wind speed. This result is consistent with the expected slick velocity with absence of surface water currents [8]. In Figure 4 the two slicks have been superimposed along with the average wind field (5 m/s) to show their evolution as captured by the three sensors.
The same tracking analysis has been carried out for the slick detected on 4th September. Although the position of this slick is very near to that detected on 30th–31th August, it is very likely that we are concerned with a different spill. In fact, the distance between the two patterns is about 10 km, while in 24 hours (from 30th to 31st August) a movement of 17 km has been recorded. In Figure 5 is shown a detail of the three acquisitions of the slick with the wind field superimposed. The displacement between the ASAR and the MODIS Terra oil slick is about 700 m, for an average velocity of 0.19 m/s. As the slick's drift direction resulted opposite to the wind direction, it can be assumed the action of a sea surface current to explain the observations. Instead, the separation measured on MODIS Terra and MODIS Aqua acquisitions

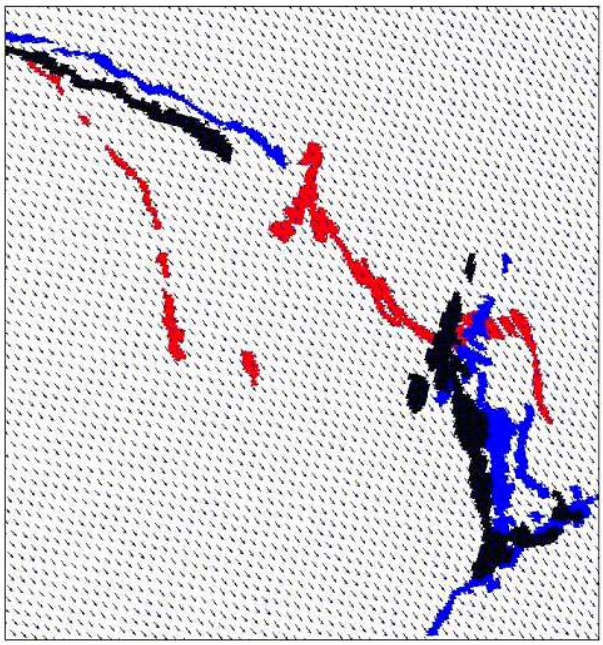

Figure 4. The two probable oil slicks detected offshore Crete on 30th–31 August 2004 by MERIS (black), MODIS Terra (red) and MODIS Aqua (blue) are superimposed on the same grid to highlight their shape evolution. The average wind field is also superimposed. It can be seen that the slicks movement is consistent to the wind vectors.

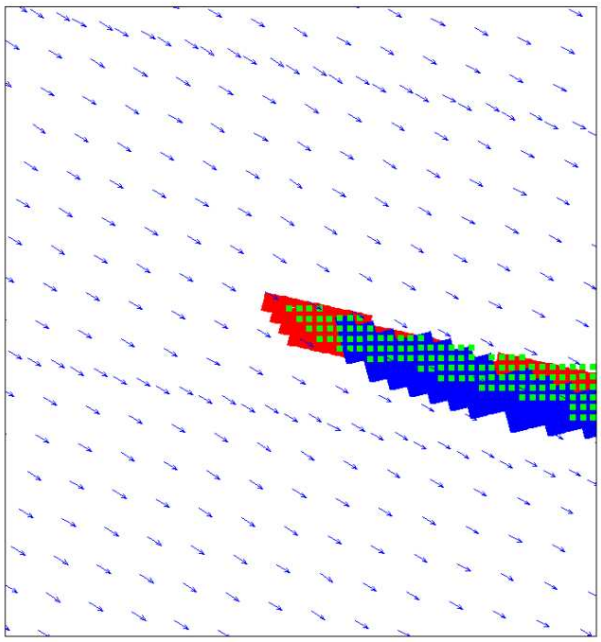

Figure 5. Composite of the slicks observed on 4st September 2004 from ASAR (green), MODIS Terra (red) and MODIS Aqua (blue) with superimposed the average wind field. As the drift of the slick is not consistent with the wind direction, the effect of a sea surface current could be envisaged.

is about 2.5 km, to which corresponds an average velocity of about 0.44 m/s, i.e. about 9% the wind speed (5 m/s), thus strengthening the assumption that the action of a water current should be considered to explain the observed movement. It should also be pointed out that these short term drift measurements are affected by a localization error of the order of the pixel size (about 300 m); beside, the banding artefact of the MODIS Aqua image introduces a further source of error, which is comparable to the distances travelled by the slick.

4. CONCLUSIONS

A method supporting and extending SAR capability to detect marine oil spills that exploits VIS/NIR imagery provided by MERIS, MODIS Terra and MODIS Aqua satellite platforms of the sea surface under sunglint imaging conditions has been developed.
The impact of atmospheric effects on the detection of oil spill features has been evaluated using a refined reflectance modelling based on the vectorial radiative transfer code "6S". The procedure has been applied to oil spills in the Mediterranean Sea offshore Crete island during August and September 2004.
The separability of the oil slick and consequently its detection improves, especially if the atmospheric contribution is taken into account, using a ratio image properly defined.
Due to the high temporal rate of satellite optical acquisitions, the possibility to track the movement of the detected oil slicks is feasible. The expected mean drift velocity, usually equal to $3 - 5\%$ of the wind speed when the sea surface currents are negligible [8], has been verified for one of the two presented cases. The other case study shows a manifest contribution of water current that can be accounted for only if a detailed current model is available. Considering the geolocation errors (up to 300 m for MODIS [9] and MERIS [10]), the uncertainty on wind speed (about 2 m/s [11] for SAR wind retrieval and about 3 m/s for ECMWF predictions [7]), the image measurements can be considered fairly accurate in view of an operative surveillance service.

5. ACKNOWLEDGMENTS

The ENVISAT ASAR and MERIS images used for this study were provided by ESA within the CAT-1 project 3506 "Exploitation of MERIS images for oil spill detection".

REFERENCES

[1] Cox C., Munk W., 1954, Measurement of the roughness of the sea surface from photographs of the sun's glitter, J. Opt. Soc. Am., 44, 838-850

[2] Cox C., Munk W., 1956, Slopes of the sea surface deduced from photographs of sun glitter, Bull. Scripps Inst. Oceanography, vol. 6, n. 9, 401-488

[3] Chandrasekhar S., 1960, Radiative Transfer, Dover Pubblication

[4] Vermote E.F., Tanre D., Deuze J.L., Herman M., Morcette J.J., 1997, Second Simulation of the Satellite Signal in the Solar Spectrum, 6S: An overview, IEEE Trans. Geosci. and Rem. Sens., vol. 35, n. 3, 675-686

[5] Tanre D., Herman M., Deschamps P.Y., 1983, Influence of the atmosphere on space measurements of directional properties, Applied Optics, vol. 22, n. 5, 733-741

[6] Adamo M., De Carolis G., De Pasquale V., Pasquariello G., 2005, Combined use of SAR and Modis imagery to detect marine oil spills, Proc. EOS/SPIE Symposium in Remote Sensing

[7] Portabella M., Stoffelen A., Johannessen J.A., 2002, Toward an optimal inversion method for synthetic aperture radar wind retrieval, J. Geophys. Res., vol. 107, 10.1029/2001JC000925

[8] Bern T.I., 1993, Norwegian slick study, Vol. 1 oil slick study, Oceanor, Trondheim, Norway, Vol. OCN R-93080

[9] Wolfe R., Nishima M., Kuyper J., 2006, Improving satellite moderate resolution instrument geolocation accuracy in rough terrain, http://modis.gsfc.nasa.gov/sci_team/meetings/200610/presentations/posters/wolfe1.pdf

[10] Goryl P., Saunier S., 2004, Meris absolute geolocation status, http://earth.esa.int/pcs/envisat/meris/documentation/GAEL-P179-TCN-006-01-00-Meris_Absolute_location_control_report.pdf

[11] Holt B., 2004, Wave refraction, breaking, and other near-shore processes, Synthetic Aperture Radar Marine User's Manual, U.S. Dept. of Commerce, Washington, D.C., 25-79